7920 *Biochemistry* **2010,** *49,* 7920–7929
DOI: 10.1021/bi100729m

BIOCHEMISTRY
including biophysical chemistry & molecular biology
Article

Cell-Selective Lysis by Novel Analogues of Melittin against Human Red Blood Cells and *Escherichia coli*†

Brijesh K. Pandey,[‡,∥] Aqeel Ahmad,[‡,∥] Neeta Asthana,[‡,∥] Sarfuddin Azmi,[‡] Raghvendra M. Srivastava,[‡] Saurabh Srivastava,[‡] Richa Verma,[‡] Achchhe Lal Vishwakarma,[§] and Jimut Kanti Ghosh*[,‡]

[‡]*Molecular and Structural Biology Division,* [§]*Sophisticated Analytical Instruments Facilities, and Central Drug Research Institute, CSIR, Lucknow 226001, India* [∥] *These authors have contributed equally to this work*

Received May 8, 2010; Revised Manuscript Received August 7, 2010

ABSTRACT: Melittin is a good model antimicrobial peptide to understand the basis of its lytic activities against bacteria and mammalian cells. Novel analogues of melittin were designed by substituting the leucine residue(s) at the "d" and "a" positions of its previously identified leucine zipper motif. A scrambled peptide having the same composition of melittin with altered leucine zipper sequence was also designed. The analogues of melittin including the scrambled peptide showed a drastic reduction in cytotoxicity though they exhibited comparable bactericidal activities. Only melittin but not its analogues localized strongly onto hRBCs and formed pores of ∼2.2−3.4 nm. However, melittin and its analogues localized similarly onto *Escherichia coli* and formed pores of varying sizes as tested onto *Bacillus megaterium*. The data showed that the substitution of hydrophobic leucine residue(s) by lesser hydrophobic alanine residue(s) in the leucine zipper sequence of melittin disturbed its pore-forming activity and mechanism only in hRBCs but not in the tested bacteria.

Peptides with lytic activities against different cells often contribute in the defense mechanisms and offensive actions of many organisms (*1*, *2*). Melittin is one such peptide, which is the major component of honey bee, *Apis mellifera* venom (*3*, *4*). This 26-residue amphipathic peptide possesses a broad spectrum of lytic activities against a variety of cells (*5*−*12*). The mechanism of melittin-mediated lysis is associated with the membrane permeabilization of target cells, which causes the leakage of cell contents and leads to a breakdown of the transmembranal potential and ion gradients (*4*, *13*−*19*). The mechanism of membrane interaction of melittin has been analyzed in detail by studying its phospholipid membrane interactions with different kinds of lipid compositions (*12*, *20*−*23*). The structural studies have been performed with melittin by both NMR (*24*−*28*) and X-ray crystallography (*29*, *30*). The crystal structure of melittin shows a tetrameric structure in the presence of high salt (*30*).

The broad-spectrum lytic activity of melittin against a large number of microorganisms makes it a potential lead molecule for developing novel antimicrobial agents. There have been numerous structure−function studies and number of efforts to design analogues of melittin with reduced toxic activities (*5*, *14*, *31*−*34*). Very recently, a diastereomer of melittin, designed by deletion of the central hinge region and C-terminal glutamines along with incorporation of a few D-amino acids, has been reported to exhibit significantly reduced hemolytic activity in comparison to melittin (*35*). Previously, a leucine zipper-like motif was identified in melittin (*36*). It was shown that the motif plays a crucial role in controlling the hemolytic activity of melittin but apparently not in its antibacterial activity. The mutations at the heptadic "a" positions drastically reduced the hemolytic activity of melittin but not its antibacterial activity against several selected Gram-positive and -negative bacteria. Interestingly, the double alanine-substituted analogue of melittin has been recently demonstrated to attenuate the epithelial permeation enhancement activity of melittin, and it was concluded that the attenuation is correlated with reduced cytotoxicity (*37*). Furthermore, the role of this sequence element has been shown in determining the cytotoxic activity of cathelicin-derived antimicrobial peptides, BMAP-28 and BMAP-27 (*38*, *39*). Novel analogues of naturally occurring antimicrobial peptides have been designed by mutating the specific amino acids of this structural element (*40*).

However, despite detailed studies it is not clearly known how these melittin analogues exhibited contrasting antibacterial and hemolytic activity against the bacteria and human red blood cells and what is their mechanism of action. Interestingly, melittin possesses leucine residues at both the "a" and "d" positions of its heptad repeats. Since the "d" positions of the heptad repeat sequence also play an equally crucial role in the assembly of the parent molecule (*41*−*43*), we decided to look into the effect of similar amino acid substitutions at the "d" positions of the heptad repeat of melittin. For this purpose several novel analogues of melittin, in which leucine residue(s) at "d" position(s) of the heptad repeat was (were) replaced with single and double alanine residue(s), were synthesized and characterized. Furthermore, a novel analogue with amino acid substitutions at both "a" and "d" positions and a scrambled melittin analogue having the same amino acid composition as melittin but with impaired leucine zipper sequence were also designed in the present study. In order to understand the basis of antibacterial and cytotoxic

†This work was supported by a Council of Scientific and Industrial Research (CSIR) network project NWP 0005. B.K.P., A.A., N.A., S.A., and R.V. acknowledge the receipt of SRFs, and S.S. acknowledges the receipt of JRF from CSIR, India.

*To whom correspondence should be addressed. Tel: 091-522-2612411-18 (ext 4282). Fax: 091-522-2623405. E-mail: jighosh@yahoo.com.

 Published on Web 08/09/2010

activities of melittin and its analogues, localization of these peptides onto hRBCs[1] and *Escherichia coli* and permeabilization of these cell membranes were studied. Also, the peptide-induced permeabilization of lipid vesicles, which mimics the mammalian and bacterial cell membranes, was examined. Moreover, the sizes of the pores induced by melittin and its analogues onto *Bacillus megaterium* and hRBCs were determined in order to understand the plausible mechanism of antibacterial and cytotoxic activity of melittin and its analogues.

MATERIALS AND METHODS

Materials. Rink amide MBHA resin (loading capacity, 0.63 mmol/g) and all of the N-α Fmoc and side-chain protected amino acids were purchased from Novabiochem, Switzerland. Coupling and other reagents for solid-phase peptide syntheses and cleavage of peptides from the resin as reported before were purchased either from Sigma, India, or from reputed local companies. Acetonitrile (HPLC grade) was procured from Merck, India. FITC-dextrans were purchased from Sigma, India. Tetramethylrhodamine succinimidyl ester (Rho) was purchased from Molecular Probes (Eugene, OR). The rest of the reagents were of analytical grade and procured locally; buffers were prepared in milli Q water.

Peptide Synthesis, Fluorescent Labeling, and Purification. Stepwise solid-phase syntheses of all the peptides, labeling of the peptides onto the resins, cleavage of these unlabeled and labeled peptides from the resins, and their purification by reverse-phase HPLC were achieved by standard procedures as described earlier (*36*, *44*−*46*). The purified peptides were ∼95% homogeneous, and the experimental molecular mass of the peptides, detected by ES-MS analysis, corresponded very close to the desired values. The concentrations of the peptides were determined by measuring their absorbance at 280 nm in 6 M guanidine hydrochloride with the help of the tryptophan extinction coefficient of 5690.

Assay of Hemolytic Activity of the Peptides. Hemolytic activity of melittin and its analogues was assayed by a standard procedure as reported earlier (*33*, *36*). Fresh human red blood cells (hRBCs) were washed three times in PBS. Peptides, dissolved in water, were added to the suspension of hRBCs (6% final, v/v) in PBS to the final volume of 200 μL and incubated at 37 °C for 35 min. After the samples were centrifuged, the release of hemoglobin was monitored by measuring the absorbance (A_{sample}) of the supernatant at 540 nm. For negative and positive controls hRBCs in PBS (A_{blank}) and in 0.2% (final concentration, v/v) Triton X-100 (A_{Triton}) were used, respectively. The percentage of hemolysis was calculated according to the equation:

$$\% \text{ hemolysis} = [(A_{sample} - A_{blank})/(A_{Triton} - A_{blank})] \times 100$$

Antibacterial Activity Assay of the Peptides. This bioassay with melittin and its analogues was done in 96-well microtiter plates against Gram-positive bacteria, *Bacillus subtilis* ATCC 6633 and *Staphylococcus aureus* ATCC 9144, and Gram-negative bacteria, *E. coli* ATCC 10536 and DH5α (*33*, *39*). In brief, bacteria were grown at 37 °C with shaking at 180 rpm in appropriate growth medium to the midlog phase as determined by the optical density at 600 nm, which was 0.4−0.5; subsequently 50 μL of bacterial culture was added to 50 μL of water containing 2-fold serially diluted different peptides in each well and incubated for 18−20 h at 37 °C. The peptides' antibacterial activities, expressed as their MICs (the peptide concentration which results in 100% inhibition of microbial growth), were assessed by measuring the absorbance at 600 nm.

Confocal Microscopic Experiments. Localization and binding of the peptides onto the hRBCs and *E. coli* 10536 were studied using the rhodamine-labeled versions of melittin and its analogues by employing a Zeiss LSM-510 META confocal microscope using a 63 × 1.4 NA (oil) Plan apochromate lens. Fresh hRBCs (6% in PBS) as used in peptide hemolytic activity assays were incubated with 2 μM rhodamine-labeled melittin and its analogues for 10 min at 37 °C. Cells were washed and fixed with 2% paraformaldehyde (10 min) after extensive washing with PBS, and then confocal microscopic images of cells were taken with an argon ion laser set for Rho excitation at 561 nm. The setting of the photomultiplier was constant during the whole experiments (*39*).

Localization and binding of the peptides onto the bacterial cells were also examined with the help of Rho-labeled peptides by employing a confocal microscope. *E. coli* (∼10^6 CFU/mL) in LB medium were incubated in the absence and presence of rhodamine-labeled melittin and its analogues at their MICs for half an hour and then centrifuged, washed, and analyzed by the confocal microscope as described above.

Assay of Peptide-Induced Depolarization of hRBC and E. coli Cell Membrane. Peptide-induced depolarization of the hRBC and *E. coli* 10536 membrane was detected by its efficacy to dissipate the potential across these cell membranes (*12*, *38*, *39*, *47*). Fresh human red blood cells were collected in the presence of an anticoagulant from a healthy volunteer and washed three times in PBS and resuspended in the same buffer with a final cell volume of 0.6% (v/v). The bacteria were grown at 37 °C until they reached to their midlog phase and centrifuged followed by washing with buffer (20 mM glucose, 5 mM HEPES, pH 7.3). Then bacteria were resuspended (final ∼2 × 10^5 CFU/mL) in the similar buffer containing 0.1 M KCl. Both hRBCs and bacteria were incubated with diS-C_3-5 probe for 1 h. When the fluorescence level (excitation and emission wavelengths set at 620 and 670 nm, respectively) of the hRBCs or bacterial suspension became stable, different amounts of each of the peptides were added to these suspensions in order to record the peptide-induced membrane depolarization of either hRBCs or bacterial membrane. Membrane depolarization as measured by the fluorescence recovery (F_t) was defined by the equation (*12*, *47*) $F_t = [(I_t - I_0)/(I_f - I_0)] \times 100$, where I_f, the total fluorescence, was the fluorescence levels of cell suspensions just after addition of diS-C_3-5, I_t was the observed fluorescence after the addition of a peptide at a particular concentration either to hRBCs or to *E. coli* suspensions, which were already incubated with diS-C_3-5 probe for 1 h, and I_0 was the steady-state fluorescence level of the cell suspensions after 1 h incubation with the probe.

Assay of Peptide-Induced Depolarization of Lipid Vesicles. Melittin and its analogues' induced disturbance of membrane bilayer was measured by their ability to dissipate the diffusion potential across the membrane in the presence of zwitterionic PC/Chol (8:1 w/w) and negatively charged PC/PG (7:3 w/w) lipid vesicles. Small unilamellar vesicles were prepared in K^+ buffer (50 mM K_2SO_4/25 mM HEPES−sulfate, pH 6.8) by

[1]Abbreviations: FITC, fluorescin isothiocyanate; hRBC, human red blood cell; PBS, phosphate-buffered saline; Rho, tetramethylrhodamine; CFU, colony forming units; Fmoc, *N*-(9-fluorenyl)methoxycarbonyl; DIC, differential interference contrast; Chol, cholesterol; HPLC, high-performance liquid chromatography; PC, egg phosphatidylcholine; PG, egg phosphatidylglycerol; MALDI-TOF, matrix-assisted laser desorption ionization time of flight; MICs, minimum inhibitory concentrations; PI, propidium iodide; PEG, poly(ethylene glycol).

ultrasonication in a bath-type sonicator (Laboratory Supplies Co., New York); afterward, appropriate amounts of the lipid vesicles were suspended in isotonic (K^+-free) Na^+ buffer (50 mM Na_2SO_4/25 mM HEPES−sulfate, pH 6.8) followed by the addition of the potential sensitive dye diS-C_3-5. Addition of the K^+-selective ionophore valinomycin to the lipid vesicles caused efflux of these ions, thereby developing a potential gradient across the lipid bilayer resulting in a polarized state which in turn quenched the fluorescence of the dye. When the dye exhibited a steady fluorescence level, peptides were added. Membrane permeability of the peptides was detected by the increase in fluorescence of the dye, which resulted from the dissipation of diffusion potential. The peptide-induced dissipation of diffusion potential was measured in terms of percentage of fluorescence recovery (F_t) by the same equation as shown in the previous section of assay of peptide-induced depolarization of hRBC and bacteria. Here I_t = the observed fluorescence after the addition of a peptide at time t (~5 min after the addition of the peptide), I_0 = the fluorescence after the addition of valinomycin, and I_f = the total fluorescence observed before the addition of valinomycin. Excitation and emission wavelengths of diS-C_3-5 and excitation and emission slits were the same as above.

Circular Dichroism Experiments. CD spectra of melittin and its analogues were recorded in the presence of phospholipid vesicles by utilizing a Jasco J-810 spectropolarimeter as reported before (*36*, *39*, *44*). The samples were scanned at room temperature (~30 °C) in a capped quartz cuvette of 0.20 cm path length in the wavelength range of 250−195 nm.

Osmotic Protection Assay. To determine the diameter of the pores formed by melittin on hRBCs, hemolytic activity of melittin was examined in the presence of osmotic protectors as described previously (*48*−*51*) with 3% (final concentration, v/v) hRBCs. Human erythrocytes, prepared in the same way as the previous experiment, were suspended in PBS and incubated with one of the following osmotic protectors at 30 mM concentration at 37 °C. Raffinose, poly(ethylene glycol) (PEG) 1500, PEG 2000, PEG 3350, PEG 4000, and PEG 6000 of diameters 1.3, 2.2, 2.5, 3.4, 4, and 4.9 nm, respectively, were used in this experiment as osmotic protectors. After 30 min of incubation to each of the protector-treated erythrocytes, 4.2 μM melittin was added. Melittin-induced hemolysis was determined after another incubation of 50 min at 37 °C by recording the absorbances of the supernatants at 540 nm as the hemolytic activity assay experiment. When the size of the osmotic protector matches with the size of pores formed by melittin onto the hRBC, inhibition of the hemolytic activity of the peptide is observed. Thus, by observing inhibition of hemolysis in the presence of osmotic protectors, a probable diameter of the pore formed by melittin onto the hRBC was determined.

Determination of Peptide-Induced Pore in B. megaterium by Confocal Microscopy. Entry of FITC-dextran in bacteria was performed with slight modification in the protocol of Imura et al. (*52*). Soluble FITC-dextran of 40, 70, and 250 kDa was used to determine the diameter of the pores formed in *B. megaterium* (NRRL B-4272) in the presence of melittin and its designed analogues. Cells were grown up to 10^6 CFU/mL and washed with PBS three times to remove the media component, and 10^5 cells were incubated in 24-well plates along with FITC-dextran of 40, 70, and 250 kDa at 0.16 mg/mL. Concentration of each of the peptides was 4 μM. In the control experiment no peptide was added. After 30 min incubation cells were transferred to microcentrifuge tubes and washed with PBS to remove free FITC-dextran. Finally, cells were transferred to a polylysine-coated glass slide for observation under a Zeiss LSM 510 Meta confocal laser scanning microscope.

Experimental procedures to measure tryptophan blue shifts of melittin and its analogues in the presence of zwitterionic and negatively charged lipid vesicles have been described in the Supporting Information (Figure S1), whereas the experimental details of detection of peptide-induced membrane damage of hRBC and *E. coli* by flow cytometry have been described in the Supporting Information (Figures S4 and S5).

RESULTS

Design of Novel Analogues of Melittin. The present work was aimed at the designing of novel cell-selective analogues of melittin and understanding their mechanism of action by studying directly the interaction of these peptides with hRBC and the bacterium *E. coli* 10536. Previously, we identified a leucine zipper motif in melittin, and the effect of substitution of leucine residue(s) by alanine residue(s) at the heptadic position(s) ("a") on its antibacterial and hemolytic activities and phospholipid membrane interaction was analyzed (*36*). However, it was not known how the substitution of amino acids at the equally important "d" positions influences the activity of melittin. Therefore, three novel analogues, namely, (L9A) melittin, (L16A) melittin, and (L9,16A) melittin, were designed after substituting single and double amino acid residues at "d" positions of the heptad repeat of melittin. Besides an analogue, (L9,13A) melittin was designed in which leucine residues at a "d" and an adjacent "a" position of melittin were substituted by alanine residues. Furthermore, a scrambled melittin analogue (melittin scrambled) having the identical composition of melittin but with impaired leucine zipper sequence was designed. The scrambled peptide contained alanine, valine, and glycine instead of leucine residues at two "a" positions and one "d" position of the heptad repeat of melittin; the isoleucine residue at the other "d" position (16th) was unchanged. Though melittin scrambled possesses an impaired leucine zipper sequence, it contains a similar hydrophobic face like the parent molecule as indicated by the Schiffer and Edmundson wheel projections of 1−18 residues of melittin and its scrambled analogue (Figure 1A). All of the designed melittin analogues including the scrambled peptide contain the same number of charged residues with their positions remaining intact as in melittin. Figure 1B also depicts the mean hydrophobicity and mean hydrophobic moments of these peptides in Eisenberg's scale, which shows a minor variation in mean hydrophobic moments among the peptides. While melittin and its scrambled analogue possess the same mean hydrophobicity, there are only slight differences between melittin and its alanine-substituted analogues in their mean hydrophobicity values. The molecular masses of the peptides determined by ES-MS analysis were very close to their theoretical values (Figure 1B).

Substitution of Leucine by Alanine at the "d" Position of the Heptad Repeat Significantly Reduced the Hemolytic Activity of Melittin against the Human Red Blood Cells. The effect of substitution of leucine residue(s) at "d" position(s) of the melittin heptad repeat on its toxic activity was investigated by measuring the hemolytic activity of the peptides against the human red blood cells (hRBCs). As shown in Figure 2, the hemolytic activity of melittin analogues in which a single leucine residue at "d" position was substituted by a single alanine residue [(L9A) melittin and (L16A) melittin] exhibited significantly reduced hemolytic activity than that of melittin. The hemolytic

A

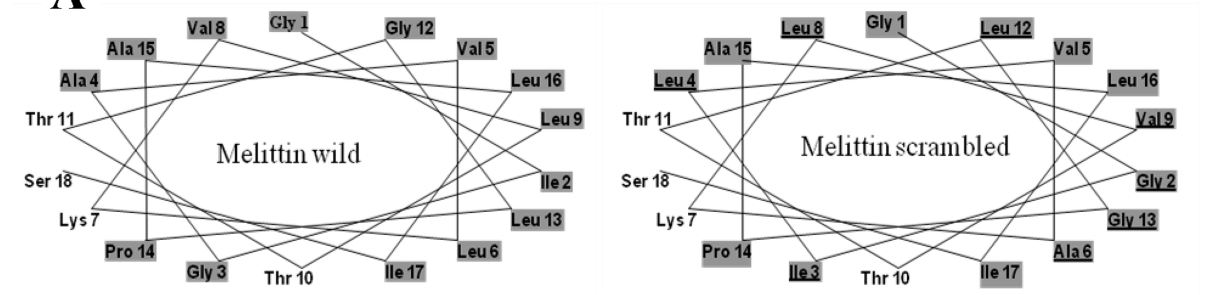

B

Peptide	Sequence (X = H or Rho)	Calculated mass	Observed mass	<H>	μ
	abcdefgabcdefga				
Melittin wild	X-NH-GIGAV**L**KV**L**TTG**L**PA**L**ISW**I**KRKRQQ-CONH$_2$	2846.44	2846	-0.08	0.22
(L9A) Melittin	X-NH-GIGAV**L**KV**A**TTG**L**PA**L**ISW**I**KRKRQQ-CONH$_2$	2803.69	2803.93	-0.09	0.21
(L16A) Melittin	X-NH-GIGAV**L**KV**L**TTG**L**PA**A**ISW**I**KRKRQQ-CONH$_2$	2804.36	2805	-0.09	0.21
(L9,16A) Melittin	X-NH-GIGAV**L**KV**A**TTG**L**PA**A**ISW**I**KRKRQQ-CONH$_2$	2762.28	2762.25	-0.1	0.2
(L9,13A) Melittin	X-NH-GIGAV**L**KV**A**TTG**A**PA**L**ISW**I**KRKRQQ-CONH$_2$	2762.28	2763	-0.1	0.2
Melittin Scrambled	X-NH-G**GIL**V**A**K**LV**TT**LG**PA**L**ISW**I**KRKRQQ-CONH$_2$	2846.44	2847	-0.08	0.18
Amino acids at the a- and d-positions are shown in boldface, and substituted amino acids are shown in boldface and underlined, <H> and μ denotes mean hydrophobicity and hydrophobic moment of the peptides respectively, calculated using Eisenberg's scale of hydrophobicity.					

FIGURE 1: (A) Schiffer and Edmundson helical wheel projections of 1−18 residues of melittin wild and melittin scrambled, hydrophobic residues are shown in shaded font; mutated positions in melittin scrambled are shown as underlined. (B) Amino acid sequence, calculated mass, observed mass, mean hydrophobicity, and hydrophobic moments of melittin and its designed analogues.

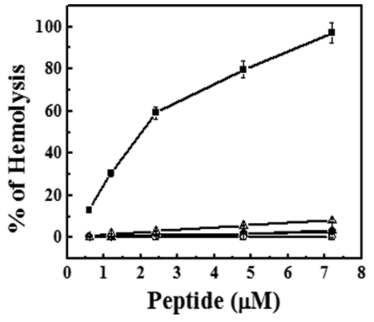

FIGURE 2: Dose-dependent hemolytic activity of melittin and its designed analogues. Symbols: solid square, melittin; solid circle, (L9A) melittin; solid triangle, (L16A) melittin; open square, (L9,16A) melittin; open circle, (L9,13A) melittin; open triangle, melittin scrambled. Each point represents the mean result of three independent experiments, and the error bar indicates the standard deviation.

activity of the analogues in which two leucine residues either at two "d" positions [(L9,16A) melittin] or at one "d" and one "a" [(L9,13A) melittin] position were substituted by two alanine residues further reduced and showed practically no hemolysis at the maximum concentration examined here. Thus the results showed that the substitution of amino acids at the "d" positions drastically reduced the hemolytic activity of melittin as was also observed in the case of amino acid substitution at the "a" positions (*36*). The hemolytic activity of the double alanine-substituted analogues with one "d" and one "a" and two "d" amino acid substitutions was indistinguishable. Interestingly, melittin scrambled having the same amino acid composition and very similar hydrophobic face as melittin but with impaired leucine zipper sequence also exhibited drastically reduced

Table 1: Antibacterial Activity of Melittin and Its Analogues

	MIC[a] (μM)			
peptide	*E. coli* DH5α	*E. coli* ATCC 10536	*S. aureus* ATCC 9144	*B. subtilis* ATCC 6633
melittin wild	3.8 ± 0.5	3.8 ± 0.5	3.6 ± 0.4	3.9 ± 0.5
(L9A) melittin	4.3 ± 0.5	3.2 ± 0.4	3.6 ± 0.4	2.4 ± 0.3
(L16A) melittin	4.2 ± 0.5	4.1 ± 0.5	4.2 ± 0.5	3.9 ± 0.5
(L9,16A) melittin	4.2 ± 0.5	3.3 ± 0.4	4.0 ± 0.5	6 ± 0.3
(L9,13A) melittin	4.3 ± 0.5	4.5 ± 0.5	> 20	> 20
melittin scrambled	4.8 ± 0.4	4.7 ± 0.5	5.0 ± 0.6	5.8 ± 0.6

[a]MIC values are the mean of three independent experiments each performed in duplicate ± the standard deviation.

hemolytic activity, supporting a crucial role of the hydrophobic leucine residues at the "a" and "d" positions of melittin's heptad repeat sequence.

The Analogues of Melittin Exhibited Comparable Antibacterial Activity to Melittin. The antibacterial activities of melittin and its analogues against the selected bacteria were assayed in liquid culture to determine their antibacterial activities. As shown in Table 1, the analogues of melittin showed comparable antibacterial activities to melittin against the selected Gram-positive and -negative bacteria. Thus the results suggested that, unlike the hemolytic activities of the peptides, the melittin analogues significantly retained the antibacterial activities of the wild-type peptide. However, it is to be mentioned that of these melittin analogues, though (L9,13A) melittin appreciably retained the bactericidal activity against the Gram-negative bacteria, it showed much lower activity against the tested Gram-positive

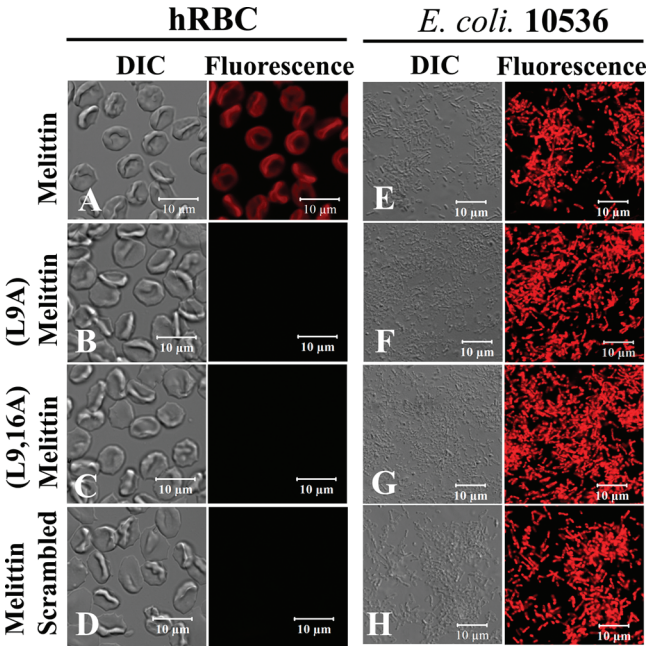

FIGURE 3: Detection of localization of the Rho-labeled melittin, (L9A) melittin, (L9,16A) melittin, and melittin scrambled onto hRBCs and *E. coli* 10536 cells by confocal microscopy. Each cell type has been marked on top of the images, and Rho-labeled peptides that have been used to treat the cells are shown on the left-hand side. For each of the peptide treatments, DIC and fluorescence images of each cell type have been shown. Peptide concentration of each of the Rho-labeled peptides for treatment with hRBCs was ~2.0 μM whereas for treatment with *E. coli* was ~3.0 μM.

bacteria as compared to the other peptides, the reason of which is not clearly understood at present.

Significant Differences in the Localization of Melittin and Its Analogues onto Human Red Blood Cells but Not to E. coli. The effect of substitution of leucine residue(s) by alanine residue(s) in the leucine zipper sequence of melittin on its localization onto hRBCs and *E. coli* 10536 was studied with the help of fluorescent-labeled peptides utilizing a confocal microscopic technique. Red fluorescence of Rho-labeled melittin was clearly prominent onto the hRBCs, indicating a strong binding of Rho-melittin molecules onto these cell membranes (Figure 3A). However, the red fluorescence onto hRBCs decreased significantly when Rho-labeled melittin was replaced with Rho-labeled (L9A) melittin or (L9,16A) melittin or melittin scrambled (Figure 3, panels A−D). The results clearly suggested that the substitution of hydrophobic leucine residues at single or double "d" position(s) of the melittin heptad repeat by lesser hydrophobic alanine residues drastically decreased its binding onto hRBCs. Even melittin scrambled with the same amino acid composition as melittin but with impaired leucine zipper sequence bound to hRBCs weakly.

However, when the same experiment was performed onto *E. coli*, red fluorescence of Rho-labeled melittin and its analogues was observed to a similar extent onto the bacteria (Figure 3, panels E−H). The data clearly suggested a comparable binding and localization of these peptides onto bacterial cells. Unlike in the case of localization of these peptides onto hRBCs, leucine to alanine substitution did not affect the binding of melittin to *E. coli*. Besides, these images showed an appreciable number of bacteria with altered morphology following the treatment of Rho-labeled melittin and its selected analogues. The data suggest that probably these peptides target the bacterial membrane in order to exhibit their antibacterial properties, and labeling of these peptides by the fluorescent probe did not significantly affect their membrane damaging activities. Altogether, the confocal microscopic studies indicated that the substitution of leucine residue(s) by alanine residue(s) showed a significant effect only on the binding and localization of melittin onto hRBCs but not onto *E. coli*.

Furthermore, the relative localization of tryptophan residues of melittin and its analogues onto bacterial and mammalian cell membrane mimetic model membranes was studied by recording the shift of their tryptophan emission maxima toward the shorter wavelength (blue shift) in the presence of PC/PG (7:3 w/w) and PC/Chol (8:1 w/w) lipid vesicles, respectively. Melittin as well as all of its alanine-substituted analogues exhibited a significant blue shift of tryptophan emission maxima of 18−20 nm in the presence of negatively charged PC/PG (7:3 w/w) lipid vesicles (Figure S1A in Supporting Information) which suggested that the tryptophan residues of these peptides were appreciably and similarly located inside this kind of phospholipid bilayer. However, in the presence of PC/Chol (8:1 w/w) lipid vesicles while melittin showed a tryptopan blue shift of ~20 nm, its analogues exhibited a blue shift only in the range of 2−7 nm (Figure S1B in Supporting Information). The results suggested that while the tryptophan residue of melittin was located most likely inside the bilayer of PC/Chol lipid vesicles, for its analogues it was located in much polar environment, probably closer to the surface of this kind of lipid vesicle.

The Analogues of Melittin Induced Significantly Lesser Depolarization in Human Red Blood Cells Than Melittin but Depolarized E. coli with Comparable Efficacy to Melittin. Since melittin is a membrane-active peptide, in order to understand the basis of contrasting antibacterial and hemolytic activities of its analogues toward the bacteria and hRBCs, peptide-induced depolarization of hRBC and *E. coli* ATCC 10536 membranes was measured. Melitiin efficiently depolarized both *E. coli* and hRBC membranes. Interestingly, the single alanine-substituted analogues induced appreciably less depolarization in the hRBCs, and the double alanine-substituted analogue induced even lesser depolarization in these cells as compared to that of melittin, which was evidenced by the corresponding fluorescence recovery data (Figure 4A). The scrambled melittin analogue also induced significantly lesser depolarization in hRBC membrane like the other analogues of melittin. In contrast, the melittin scrambled and the alanine-substituted melittin analogues showed comparable efficacy to melittin in depolarizing the *E. coli* membrane (Figure 4B) as indicated by the similar dose-dependent increase in the fluorescence recovery for each of these peptides. Altogether, the results suggested that the substitution of hydrophobic leucine residue(s) at the "d" and "d" and "d"/"a" position(s) impaired melittin's ability to depolarize the hRBC membrane but not the *E. coli* membrane. The Rho-labeled version of melittin and its analogues induced very similar membrane depolarization in both hRBC and *E. coli* cell membranes like their unlabeled versions as indicated by their comparable fluorescence recovery values (data not shown), suggesting that labeling of these peptides by the rhodamine probe did not show much influence on their membrane permeabilization properties.

The Analogues of Melittin Permeabilized the Negatively Charged Lipid Vesicles Very Similar to Melittin but Failed To Permeabilize the Zwitterionic Lipid Vesicles Appreciably. To understand the basis of contrasting differences in the permeabilization of *E. coli* and hRBC membranes by the

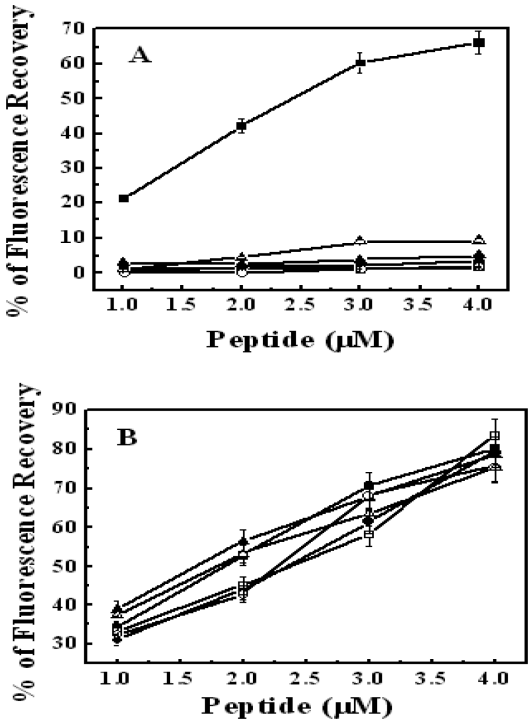

FIGURE 4: Dose-dependent peptide-induced transmembrane depolarization of human red blood and *E. coli* 10536 cell membranes. (A) Plot of the percentage of fluorescence recovery, which is a measure of peptide-induced transmembrane depolarization, vs peptide concentration in hRBCs. (B) Plot of the percentage of fluorescence recovery vs peptide concentration in *E. coli*. Symbols: solid square, melittin; solid circle, (L9A) melittin; solid triangle, (L16A) melittin; open square, (L9,16A) melittin; open circle, (L9,13A) melittin; open triangle, melittin scrambled. Each point represents the mean result of three independent experiments, and the error bar indicates the standard deviation.

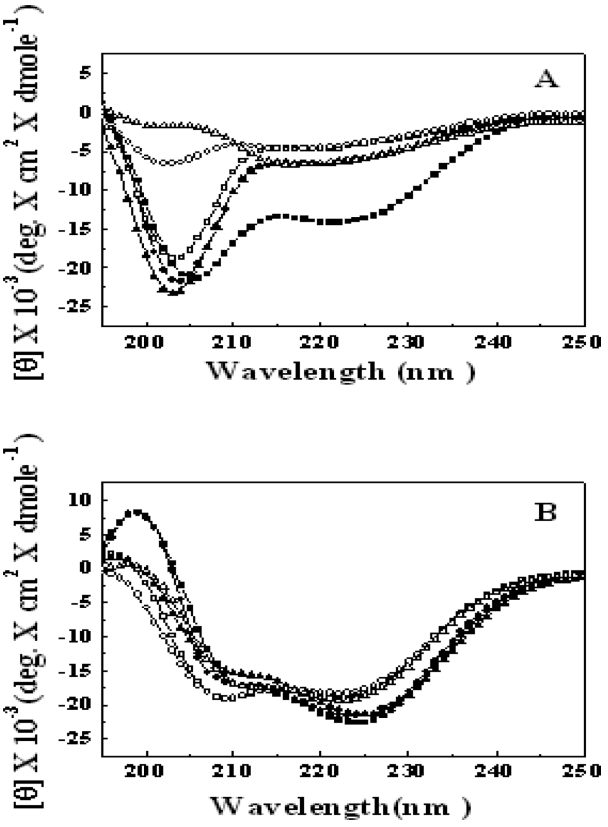

FIGURE 5: Determination of secondary structures of melittin and its analogues in the presence of (A) zwitterionic PC/Chol (8:1 w/w) vesicle, ~264 μM, and (B) negatively charged PC/PG (7:3 w/w) vesicle, ~396 μM. Concentrations of the peptides were ~21 μM. Symbols: solid square, melittin; solid circle, (L9A) melittin; solid triangle, (L16A) melittin; open square, (L9,16A) melittin; open circle, (L9,13A) melittin; open triangle, melittin scrambled.

analogues of melittin, the peptide-induced permeabilization of mammalian cell membrane mimetic, zwitterionic, PC/Chol and bacterial membrane mimetic, negatively charged, PC/PG lipid vesicles was studied. Melittin and its analogue-induced permeability of both kinds of lipid vesicles was measured with respect to the peptide-induced dissipation of diffusion potential across the phospholipid membranes by employing a potential sensitive dye as described in the Materials and Methods section. The peptide-induced dissipation of diffusion potential of a particular kind of lipid vesicles was experimentally determined by calculating the percentage of fluorescence recovery in the presence of varying concentrations of the peptides. It is clearly evident that though melittin induced significant fluorescence recovery, its analogues induced very little dissipation of diffusion potential across PC/Chol lipid vesicles (Figure S2A in Supporting Information). The data suggested that only melittin was able to permaeabilize the zwitterionic lipid vesicles while its mutants were not significantly active. Interestingly, melittin as well as its analogues induced significant and very similar fluorescence recovery in the PC/PG lipid vesicles (Figure S2B in Supporting Information), which indicated that these analogues retained the ability to permeabilize the negatively charged lipid vesicles unlike in the case of zwitterionic lipid vsicles.

The Analogues of Melittin Did Not Show Appreciable Secondary Structure in the Presence of Zwitterionic Lipid Vesicles but Adopted Similar Helical Structure to Melittin in the Presence of Negatively Charged Lipid Vesicles. Secondary structures of melittin and its designed analogues were determined in the presence of negatively charged (PC/PG, 7:3 w/w) and zwitterionic lipid vesicles (PC/Chol, 8:1 w/w) as well as in PBS (pH 7.4). Since none of the peptides exhibited appreciable secondary structure in PBS, CD spectra of the peptides in PBS have not been presented. As has been already reported (*36*), melittin adopted significant helical structure (~40%) in the presence of zwitterionic, PC/Chol lipid vesicles (Figure 5A). However, none of the melittin analogues including melittin scrambled adopted appreciable helical structure in the presence of zwitterionic, PC/Chol lipid vesicles as shown by their CD spectra. Interestingly, these alanine-substituted melittin analogues as well as melittin scrambled adopted very significant α-helical structures as melittin in the presence of negatively charged, PC/PG lipid vesicles (Figure 5B).

Melittin Formed Pores of 2.2−3.4 nm Diameter onto the Human Red Blood Cells. An osmotic protection assay against the hemolytic activity of melittin was performed in order to determine the size of the pores formed by melittin onto hRBCs. Raffinose (diameter 1.3 nm) showed no appreciable effect on the hemolytic activity of melittin against hRBCs (Figure 6). However, a decrease in hemolytic activity of melittin was observed when hRBCs were preincubated with osmotic protector PEG 1500 (diameter 2.2 nm). The inhibition of hemolytic activity of melittin increased further in the presence of PEG 2000 (diameter 2.5 nm). Maximum inhibition of melittin's hemolytic activity was observed when hRBCs were preincubated with PEG 3350 (diameter 3.4 nm). Preincubation with PEG 4000 (diameter 4 nm) and PEG 6000 (diameter 4.9 nm) showed further little

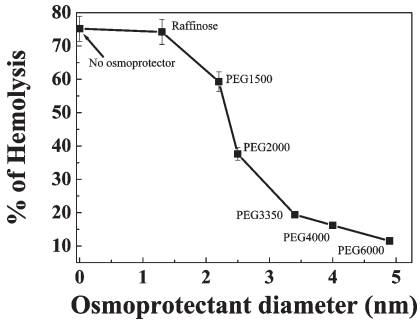

FIGURE 6: Determination of sizes of melittin-induced pores on human red blood cells by osmotic protection assay, employing different osmoprotectors as described in the Materials and Methods. Plot of percentage of melittin-induced hemolysis of hRBCs in the absence and presence of different osmoprotectors as marked in the figure. The concentration of melittin was 4.2 μM. Each point represents the mean result of three independent experiments, and the error bar indicates the standard deviation.

increase in inhibition of hemolysis. Thus the osmotic protection assay suggested that melittin formed pores onto hRBCs of diameter in the range of 2.2−3.4 nm. When PEGs were washed from the mixture of PEGs and hRBCs by PBS and then hRBCs were further incubated with melittin, hemolysis of the cells was readily observed. The result indicated that the PEGs, used in this study, acted just as osmotic protectors and not as the inhibitor of binding of the peptide to the hRBC membrane (*50*, *51*). Furthermore, flow cytometric experiments were performed by employing fluorescent-labeled peptide in order to examine the binding of melittin to hRBCs in the absence and presence of selected PEGs. It was observed that the binding of Rho-melittin to hRBCs in the presence of PEG 1500 or PEG 3500 was quite similar to the binding of the peptide to these cells in the absence of these PEGs (Figure S3 in Supporting Information). Therefore, it is clear that PEGs do not disturb the binding of melittin to hRBCs. The alanine-substituted melittin analogues and the scrambled peptide exhibited very little hemolytic activity toward hRBCs, and therefore osmotic protection assays were not attempted for these peptides.

Melittin As Well As Its Analogues Formed Pores of Similar Sizes onto B. megaterium. Due to bigger size, *B. megaterium* was chosen for this particular experiment instead of *E. coli* 10536 as used in the other experiments. The sizes of the pores formed by melittin and its analogues onto this bacterium were determined by detecting the peptide-induced entry of FITC-labeled dextran of different sizes into the bacteria by the confocal microscopic experiment. In the absence of any peptide treatment none of the FITC-labeled dextran could enter into *B. megaterium*, suggesting the intact nature of the bacterial membrane when no peptide was added (Figure 7A). However, following the treatment of melittin (Figure 7B), FITC-dextran 40 kDa (~9 nm) could easily enter into *B. megaterium* as evidenced by the intense green fluorescence of these cells. FITC-dextran 70 kDa (~11 nm) also entered into *B. megaterium* in the presence of melittin. However, the intensity of green fluorescence was less when the bacteria were incubated with FITC-dextran 250 kDa (~23 nm) following their treatment with melittin in a very similar way as in the previous experiments. It could be possible that the sizes of an appreciable fraction of the total number of pores formed by melittin onto *B. megaterium* were less than the size of FITC-dextran 250 kDa, and hence their entry was to some extent restricted into the bacteria. Taken together, the data indicated that melittin induced the formation

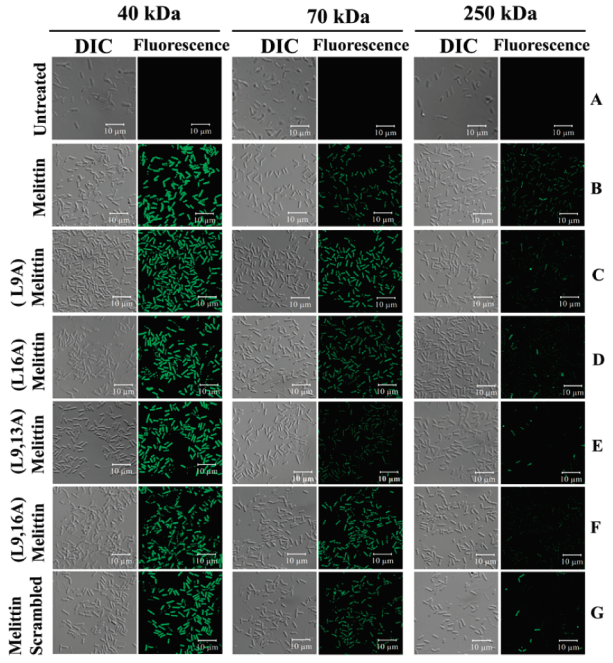

FIGURE 7: Estimation of pore sizes onto *B. megaterium* formed by melittin and its analogues. The molecular weights of FITC-dextran, used as the fluorescent size markers, have been shown on top of the respective images. Labels at the left side denote the peptides which were used to treat with *B. megaterium*. Panel A indicates bacteria treated without any peptide; panels B−G represent bacteria treated with melittin, (L9A) melittin, (L16A) melittin, (L9,16A) melittin, (L9,13A) melittin, and melittin scrambled, respectively.

of pores of variable sizes onto this bacterium; dextran of pore sizes of ~23 nm, the maximum tested here, could also enter into *B. megaterium* in the presence of melittin.

The entry of different FITC-labeled dextran was visualized onto *B. megaterium* following the treatment of bacteria with alanine-substituted melittin analogues and melittin scrambled, too. As evident from Figure 7C−G these analogues also formed pores onto *B. megaterium* which were of similar sizes to that formed by their parent molecule, melittin, onto the same bacteria.

DISCUSSION

The present study describes the design and characterization of several novel analogues of melittin after substitution of leucine by alanine residue(s) at single "d" or double "d" or one "d" and one "a" position(s) of its leucine zipper sequence. These analogues exhibited significantly reduced cytotoxicity as compared to their native molecule, melittin (Figure 2). More interestingly, a scrambled melittin analogue, which was designed by minor rearrangement in the sequence of only hydrophobic amino acids of melittin without affecting its mean hydrophobicity and also amphipathic character (Figure 1B) significantly, also exhibited drastically reduced hemolytic activity like the alanine-substituted analogues. The results clearly indicated that preserving total amino acid composition or mean hydrophobicity was not enough to maintain the cytotoxicity of melittin, and the hydrophobic leucine residues at these specific positions play a very crucial role in it. To our surprise, we found that even a melittin analogue with leucine residues at two "a" and two "d" positions substituted by equally hydrophobic valine residues also exhibited drastically reduced hemolytic activity as compared to melittin (S. Azmi and J. K. Ghosh, unpublished results), thus yielding strong evidence

to support a special role of these leucine residues in maintaining the cytotoxicity of melittin.

Interestingly, these analogues of melittin including melittin scrambled did not show significant differences with their parent molecule in the bactericidal activities (Table 1). It is to be mentioned that since alanine is also a hydrophobic amino acid, the single or double alanine-substituted melittin analogues appreciably maintain the amphipathic characters of the native peptide (Figure 1B). On the other hand, since melittin scrambled possesses the same amino acid composition as the native peptide with only minor alterations in the positions of hydrophobic amino acids, it contains a comparable hydrophobic face (Figure 1A) and amphipathicity to melittin (Figure 1B).

Consistent with the comparable bactericidal and contrasting hemolytic activity of melittin and its analogues, confocal microscopic (Figure 3) and tryptophan blue shift experiments (Figure S1 in Supporting Information) suggested a significant difference in binding and localization of melittin and its analogues onto hRBCs (Figure 3A−D) and zwitterionic lipid vesicles (Figure S1A in Supporting Information) though they were localized similarly onto *E. coli* (Figure 3E-H) or negatively charged lipid vesicles (Figure S1B in Supporting Information). Further, confocal microscopic images (fluorescence and transmission) showed that both Rho-labeled melittin and its analogues caused significant lysis and changes in the morphology of *E. coli*, suggesting that the plasma membrane of bacteria could be the target of all these peptides.

Peptide-induced depolarization and/or damage of the membrane organization of hRBCs and *E. coli* (*E. coli* 10536) cells could be related to the lysis of these cells in the presence of melittin or its analogues. The analogues of melittin did not induce appreciable permeabilization (Figure 4A) or damage of the membrane organization of hRBCs (Figure S4 in Supporting Information) though they induced significant permeabilization (Figure 4B) and damage to the membrane organization of *E. coli* (Figure S5 in Supporting Information) as that of melittin. The results probably explain the reduced cytotoxic activity of these melittin analogues against hRBCs but their comparable bactericidal activity to melittin. Melittin but not its analogues altered the membrane organization of hRBCs (Figure S4, panels B−G in Supporting Information), resulting in the exposure of phosphophatidylserine (PS) of the inner leaflet of the membrane and thus stained by the PS-binding probe annexin V-FITC (Figure S4, panel B in Supporting Information). Similar staining of hRBCs was observed in the case of *E. coli* toxin, hemolysin E-treated cells (*44*). In contrast, melittin as well as its analogues induced almost similar damage to *E. coli*, resulting in their similar staining by PI following the treatment of these peptides (Figure S5 in Supporting Information).

Since the outer membrane of hRBCs is mostly composed of zwitterionic lipids and the bacterial membrane is made of negatively charged lipids, PC/Chol (8:1 w/w) and PC/PG (7:3 w/w) were employed as mimetics of mammalian and bacterial cell membranes, respectively, in the present investigation as have been utilized by others also (*53*−*55*). A remarkable similarity was observed between the depolarization of the hRBC membrane (Figure 4A) and mammalian cell membrane mimetic, PC/Chol lipid vesicles (Figure S2A in Supporting Information) the presence of melittin and its analogues. Whereas, similar to the peptide-induced depolarization of *E. coli* (Figure 4B), melittin as well as its analogues permeabilized bacterial membrane mimetic, PC/PG lipid vesicles (Figure S2B in Supporting Information) with similar efficacy. We also previously observed (*36*) that the substitution of heptadic ("a" position) leucine residue(s) by alanine which resulted in a significant reduction in hemolytic activity of melittin without much effect on its bactericidal activity also impaired melittin-induced permeability in the zwitterionic lipid vesicles but not in the negatively charged vesicles. All of these data favor a possible strong influence of lipid−peptide interactions in determining the activity of melittin and its analogues. Moreover, the distinct lipid composition of hRBC and bacterial membranes probably plays an important role in the selective permeability of bacterial cell membrane but not the hRBC membrane by melittin analogues.

The similar extent of helical structures by melittin and its analogues in the bacterial membrane mimetic negatively charged lipid vesicles (Figure 5) could contribute in the similar permeability of *E. coli* cells in their presence and thus in their comparable antibacterial activities. Likewise, the decrease in secondary structures of these melittin analogues in the presence of mammalian cell membrane mimetic, zwitterionic lipid vesicles (Figure 5) may play a role in their reduced cytotoxicity against hRBCs.

Osmotic protection assay indicated that melittin formed pores onto hRBCs of specific sizes in the range of 2.2−3.4 nm (Figure 6). This estimated pore size on hRBC is in agreement with an earlier report on melittin-induced pore size on human erythrocytes by similar assay (*56*). It is to be mentioned that, in the toroidal-pore model (*52*, *57*, *58*), peptide helices insert into the membrane which induce the lipid monolayers to continuously bend, causing the water core to be lined by both the inserted peptides and lipid head groups giving rise to the pores with a finite size range. Magainin 2 was proposed to induce toroidal pores with an inner diameter of 3.0−5.0 nm by various reports (*59*−*61*). In another fluorescence-based study magainin 2 was proposed to form toroidal pores with an inner diameter of 2.0−3.0 and ∼3.7 nm (*62*). Thus on the basis of these previous reports, we propose that the mechanism of melittin-induced pore formation onto hRBCs was probably associated with the toroidal pore model. Neutron scattering studies on the size of pores formed by melittin onto DLPC (1,2-dilauroyl-*sn*-glycero-3-phosphocholine) bilayers also led to the toroidal pore mechanism (*61*).

Melittin and its analogues formed pores onto *B. megaterium* of variable sizes as evidenced by the entry of FITC-dextran of 9, 11, and 23 nm diameter sizes into these cells in the presence of these peptides (Figure 7). In the carpet model (*58*, *63*) of membrane disruption, a large number of peptide molecules first cover the membranes like carpet and then eventually disrupt the membrane by disturbing its bilayer curvature, which leads to the formation of micelles like the detergents. In the process of micellization, transient pores are formed in the membrane whose sizes are not well-defined. Since melittin as well as its analogues formed pores of variable sizes onto *B. megaterium* (Figure 7), it is most likely that these peptides induced permeabilization in the bacteria by the carpet mechanism. Recently, by similar experiments magainin 2 has been proposed to form pores on CHO (Chinese hamster ovary) K1 cells by the carpet mechanism since it induced the entry of FITC-dextran of different sizes (6.6−23 nm) whereas on *B. megaterium* by toroidal pore mechanism as it allowed the entry of FITC-dextrans of 2.8 nm diameter but not of 6.6 nm (*52*). There are several reports which indicate that many antimicrobial peptides including melittin form pores onto bacteria by the carpet mechanism (*22*, *58*, *63*−*66*).

A plausible structural model may be proposed on the basis of the present study for explaining the activity of melittin and its

analogues against bacteria and human red blood cells. Since the number and positions of the cationic amino acids remained intact in these melittin analogues, electrostatic interactions between these peptides and negatively charged lipids present on the outer surface of the bacterial membrane also probably remained unaffected. Since melittin and its analogues showed significant and similar helicity in the bacterial membrane mimetic, negatively charged lipid vesicles, these peptides may adopt appreciable helical structures onto the bacterial membrane and permeabilize them with comparable efficacy by utilizing the carpet mechanism, which results in their similar bactericidal activities. In contrast to bacterial membrane, the outer leaflet of mammalian cell membrane contains mostly zwitterionic lipids and lacks the acidic phospholipids. We anticipate that a strong hydrophobic interaction between the peptide molecules and these zwitterionic lipids is a prerequisite for the peptide-induced permeabilization of mammalian cell membrane. Therefore, the substitution of hydrophobic leucine residues in the "a" (*36*), "d", and both "a" and "d" position(s) by lesser hydrophobic alanine residue(s) in the leucine zipper sequence of melittin or the impairment of this structural element could significantly disturb its interaction with mammalian cell membrane. Indeed, these melittin analogues failed to adopt appreciable secondary structures in the presence of mammalian membrane mimetic, zwitterionic lipid vesicles, which could be associated to their failure to bind to hRBCs appreciably and permeabilize them by the toroidal-pore mechanism to exhibit hemolytic activity like melittin.

In summary, combining with the previous study (*36*), the results altogether suggest that the hydrophobic leucine residues either at the "a" (*36*) or "d" position possess an equally crucial role in maintaining the toxicity of melittin. Unlike the previous work (*36*), in the present report the lytic activity of melittin and its analogues against representative mammalian cell (hRBCs) and bacteria [*E. coli* 10536 (*E. coli*) and *B. megaterium* for estimation of pore sizes by confocal microscopic study] has been analyzed by directly studying their interactions with the respective cells as well as lipid vesicles mimicking the mammalian and bacterial cell membranes. Further, the mechanism of pore formation onto bacteria by these melittin analogues has been studied here which was not known before. The results depicted here strengthen the approach of design of novel, potent, cell-selective analogues of a naturally occurring cytotoxic antimicrobial peptide, melittin, by introducing a minor amino acid substitution with understanding the plausible basis.

ACKNOWLEDGMENT

Mr. Manish Singh, Electron Microscopy Unit, Central Drug Research Institute (CDRI), is thankfully acknowledged for helping us in performing confocal microscopic experiments. We thank Sanjeev Kanojiya, Sophisticated Analytical Instruments Facilities (SAIF), CDRI, for recording the ES-MS mass spectra. We are very much thankful to the anonymous reviewers for their valuable comments in improving the quality of the manuscript.

SUPPORTING INFORMATION AVAILABLE

Figure S1, determination of environment of the tryptophan residues of melittin and its analogues in the presence of different lipid vesicles; Figure S2, peptide-induced dissipation of diffusion potential across the mammalian and bacteria mimetic model membranes in dose-dependent manner; Figure S3, binding of Rho-labeled melittin to hRBCs in the absence and presence of PEGs as determined by flow cytometry; Figure S4, detection of melittin and its analogue-induced membrane damage of hRBC by FITC-annexin V staining; Figure S5, detection of melittin and its analogue-induced membrane damage of *E. coli* ATCC 10536 by PI staining. This material is available free of charge via the Internet at http://pubs.acs.org.

REFERENCES

1. Zasloff, M. (2002) Antimicrobial peptides of multicellular organisms. *Nature 415*, 389–395.
2. Boman, H. G. (1995) Peptide antibiotics and their role in innate immunity. *Annu. Rev. Immunol. 13*, 61–92.
3. Habermann, E. (1972) Bee and wasp venoms. *Science 177*, 314–322.
4. Dempsey, C. E. (1990) The actions of melittin on membranes. *Biochim. Biophys. Acta 1031*, 143–161.
5. Blondelle, S. E., and Houghten, R. A. (1991) Hemolytic and antimicrobial activities of the twenty-four individual omission analogues of melittin. *Biochemistry 30*, 4671–4678.
6. Wachinger, M., Saermark, T., and Erfle, V. (1992) Influence of amphipathic peptides on the HIV-1 production in persistently infected T lymphoma cells. *FEBS Lett. 309*, 235–241.
7. Bechinger, B. (1997) Structure and functions of channel-forming peptides: magainins, cecropins, melittin and alamethicin. *J. Membr. Biol. 156*, 197–211.
8. Winder, D., Gunzburg, W. H., Erfle, V., and Salmons, B. (1998) Expression of antimicrobial peptides has an antitumour effect in human cells. *Biochem. Biophys. Res. Commun. 242*, 608–612.
9. Diaz-Achirica, P., Ubach, J., Guinea, A., Andreu, D., and Rivas, L. (1998) The plasma membrane of *Leishmania donovani* promastigotes is the main target for CA(1−8)M(1−18), a synthetic cecropin A-melittin hybrid peptide. *Biochem. J. 330*, 453–460.
10. Herwaldt, B. L. (1999) Leishmaniasis. *Lancet 354*, 1191–1199.
11. Lazarev, V. N., Parfenova, T. M., Gularyan, S. K., Misyurina, O. Y., Akopian, T. A., and Govorun, V. M. (2002) Induced expression of melittin, an antimicrobial peptide, inhibits infection by *Chlamydia trachomatis* and *Mycoplasma hominis* in a HeLa cell line. *Int. J. Antimicrob. Agents 19*, 133–137.
12. Papo, N., and Shai, Y. (2003) New lytic peptides based on the D,L-amphipathic helix motif preferentially kill tumor cells compared to normal cells. *Biochemistry 42*, 9346–9354.
13. Tosteson, M. T., and Tosteson, D. C. (1981) The sting. Melittin forms channels in lipid bilayers. *Biophys. J. 36*, 109–116.
14. Gevod, V. S., and Birdi, K. S. (1984) Melittin and the 8−26 fragment. Differences in ionophoric properties as measured by monolayer method. *Biophys. J. 45*, 1079–1083.
15. Tosteson, M. T., Holmes, S. J., Razin, M., and Tosteson, D. C. (1985) Melittin lysis of red cells. *J. Membr. Biol. 87*, 35–44.
16. Pawlak, M., Stankowski, S., and Schwarz, G. (1991) Melittin induced voltage-dependent conductance in DOPC lipid bilayers. *Biochim. Biophys. Acta 1062*, 94–102.
17. Stankowski, S., Pawlak, M., Kaisheva, E., Robert, C. H., and Schwarz, G. (1991) A combined study of aggregation, membrane affinity and pore activity of natural and modified melittin. *Biochim. Biophys. Acta 1069*, 77–86.
18. Tanaka, H., Matsunaga, K., and Kawazura, H. (1992) ^{23}Na and ^{1}H NMR studies on melittin channels activated by tricyclic tranquilizers. *Biophys. J. 63*, 569–572.
19. Vogel, H., and Jahnig, F. (1986) The structure of melittin in membranes. *Biophys. J. 50*, 573–582.
20. Ladokhin, A. S., Selsted, M. E., and White, S. H. (1997) Sizing membrane pores in lipid vesicles by leakage of co-encapsulated markers: pore formation by melittin. *Biophys. J. 72*, 1762–1766.
21. Nir, S., and Nieva, J. L. (2000) Interactions of peptides with liposomes: pore formation and fusion. *Prog. Lipid Res. 39*, 181–206.
22. Ladokhin, A. S., and White, S. H. (2001) "Detergent-like" permeabilization of anionic lipid vesicles by melittin. *Biochim. Biophys. Acta 1514*, 253–260.
23. Gomara, M. J., Nir, S., and Nieva, J. L. (2003) Effects of sphingomyelin on melittin pore formation. *Biochim. Biophys. Acta 1612*, 83–89.
24. Brown, L. R., Lauterwein, J., and Wuthrich, K. (1980) High-resolution ^{1}H-NMR studies of self-aggregation of melittin in aqueous solution. *Biochim. Biophys. Acta 622*, 231–244.
25. Brown, L. R., and Wuthrich, K. (1981) Melittin bound to dodecylphosphocholine micelles. H-NMR assignments and global conformational features. *Biochim. Biophys. Acta 647*, 95–111.

26. Brown, L. R., Braun, W., Kumar, A., and Wuthrich, K. (1982) High resolution nuclear magnetic resonance studies of the conformation and orientation of melittin bound to a lipid-water interface. *Biophys. J. 37*, 319–328.
27. Inagaki, F., Shimada, I., Kawaguchi, K., Hirano, M., Terasawa, I., Ikura, T., and Go, N. (1989) Structure of melittin bound to perdeuterated dodecylphosphocholine micelles as studied by two-dimensional NMR and distance geometry calculations. *Biochemistry 28*, 5985–5991.
28. Ikura, T., Go, N., and Inagaki, F. (1991) Refined structure of melittin bound to perdeuterated dodecylphosphocholine micelles as studied by 2D-NMR and distance geometry calculation. *Proteins 9*, 81–89.
29. Anderson, D., Terwilliger, T. C., Wickner, W., and Eisenberg, D. (1980) Melittin forms crystals which are suitable for high resolution X-ray structural analysis and which reveal a molecular 2-fold axis of symmetry. *J. Biol. Chem. 255*, 2578–2582.
30. Terwilliger, T. C., and Eisenberg, D. (1982) The structure of melittin. II. Interpretation of the structure. *J. Biol. Chem. 257*, 6016–6022.
31. DeGrado, W. F., Kezdy, F. J., and Kaiser, E. T. (1981) Design, synthesis, and characterization of a cytotoxic peptide with melittin-like activity. *J. Am. Chem. Soc. 103*, 679–681.
32. Habermann, E., and Kowallek, H. (1970) Modifications of amino groups and tryptophan in melittin as an aid to recognition of structure-activity relationships. *Hoppe-Seyler's Z. Physiol. Chem. 351*, 884–890.
33. Oren, Z., and Shai, Y. (1997) Selective lysis of bacteria but not mammalian cells by diastereomers of melittin: structure-function study. *Biochemistry 36*, 1826–1835.
34. Boman, H. G., Wade, D., Boman, I. A., Wahlin, B., and Merrifield, R. B. (1989) Antibacterial and antimalarial properties of peptides that are cecropin-melittin hybrids. *FEBS Lett. 259*, 103–106.
35. Saravanan, R., Bhunia, A., and Bhattacharjya, S. (2010) Micelle-bound structures and dynamics of the hinge deleted analog of melittin and its diastereomer: implications in cell selective lysis by D-amino acid containing antimicrobial peptides. *Biochim. Biophys. Acta 1798*, 128–139.
36. Asthana, N., Yadav, S. P., and Ghosh, J. K. (2004) Dissection of antibacterial and toxic activity of melittin: a leucine zipper motif plays a crucial role in determining its hemolytic activity but not antibacterial activity. *J. Biol. Chem. 279*, 55042–55050.
37. Maher, S., Devocelle, M., Ryan, S., McClean, S., and Brayden, D. J. (2010) Impact of amino acid replacements on in vitro permeation enhancement and cytotoxicity of the intestinal absorption promoter, melittin. *Int. J. Pharm. 387*, 154–160.
38. Ahmad, A., Asthana, N., Azmi, S., Srivastava, R. M., Pandey, B. K., Yadav, V., and Ghosh, J. K. (2009) Structure-function study of cathelicidin-derived bovine antimicrobial peptide BMAP-28: design of its cell-selective analogs by amino acid substitutions in the heptad repeat sequences. *Biochim. Biophys. Acta 1788*, 2411–2420.
39. Ahmad, A., Azmi, S., Srivastava, R. M., Srivastava, S., Pandey, B. K., Saxena, R., Bajpai, V. K., and Ghosh, J. K. (2009) Design of nontoxic analogues of cathelicidin-derived bovine antimicrobial peptide BMAP-27: the role of leucine as well as phenylalanine zipper sequences in determining its toxicity. *Biochemistry 48*, 10905–10917.
40. Zhu, W. L., Song, Y. M., Park, Y., Park, K. H., Yang, S. T., Kim, J. I., Park, I. S., Hahm, K. S., and Shin, S. Y. (2007) Substitution of the leucine zipper sequence in melittin with peptoid residues affects self-association, cell selectivity, and mode of action. *Biochim. Biophys. Acta 1768*, 1506–1517.
41. Harbury, P. B., Kim, P. S., and Alber, T. (1994) Crystal structure of an isoleucine-zipper trimer. *Nature 371*, 80–83.
42. Greenfield, N. J., and Hitchcock-DeGregori, S. E. (1995) The stability of tropomyosin, a two-stranded coiled-coil protein, is primarily a function of the hydrophobicity of residues at the helix-helix interface. *Biochemistry 34*, 16797–16805.
43. Zhou, N. E., Kay, C. M., and Hodges, R. S. (1992) Synthetic model proteins. Positional effects of interchain hydrophobic interactions on stability of two-stranded alpha-helical coiled-coils. *J. Biol. Chem. 267*, 2664–2670.
44. Yadav, S. P., Ahmad, A., Pandey, B. K., Verma, R., and Ghosh, J. K. (2008) Inhibition of lytic activity of *Escherichia coli* toxin hemolysin E against human red blood cells by a leucine zipper peptide and understanding the underlying mechanism. *Biochemistry 47*, 2134–2142.
45. Fields, G. B., and Noble, R. L. (1990) Solid phase peptide synthesis utilizing 9-fluorenylmethoxycarbonyl amino acids. *Int. J. Pept. Protein Res. 35*, 161–214.
46. Yadav, S. P., Kundu, B., and Ghosh, J. K. (2003) Identification and characterization of an amphipathic leucine zipper-like motif in *Escherichia coli* toxin hemolysin E. Plausible role in the assembly and membrane destabilization. *J. Biol. Chem. 278*, 51023–51034.
47. Ahmad, A., Yadav, S. P., Asthana, N., Mitra, K., Srivastava, S. P., and Ghosh, J. K. (2006) Utilization of an amphipathic leucine zipper sequence to design antibacterial peptides with simultaneous modulation of toxic activity against human red blood cells. *J. Biol. Chem. 281*, 22029–22038.
48. Bhakdi, S., and Tranum-Jensen, J. (1984) Mechanism of complement cytolysis and the concept of channel-forming proteins. *Philos. Trans. R. Soc. London, Ser. B 306*, 311–324.
49. Chen, D., Kini, R. M., Yuen, R., and Khoo, H. E. (1997) Haemolytic activity of stonustoxin from stonefish (*Synanceja horrida*) venom: pore formation and the role of cationic amino acid residues. *Biochem. J. 325* (Part 3), 685–691.
50. Lange, S., Kauschke, E., Mohrig, W., and Cooper, E. L. (1999) Biochemical characteristics of Eiseniapore, a pore-forming protein in the coelomic fluid of earthworms. *Eur. J. Biochem. 262*, 547–556.
51. Yadav, S. P., Ahmad, A., Pandey, B. K., Singh, D., Asthana, N., Verma, R., Tripathi, R. K., and Ghosh, J. K. (2009) A peptide derived from the putative transmembrane domain in the tail region of *E. coli* toxin hemolysin E assembles in phospholipid membrane and exhibits lytic activity to human red blood cells: plausible implications in the toxic activity of the protein. *Biochim. Biophys. Acta 1788*, 538–550.
52. Imura, Y., Choda, N., and Matsuzaki, K. (2008) Magainin 2 in action: distinct modes of membrane permeabilization in living bacterial and mammalian cells. *Biophys. J. 95*, 5757–5765.
53. Friedrich, C. L., Rozek, A., Patrzykat, A., and Hancock, R. E. (2001) Structure and mechanism of action of an indolicidin peptide derivative with improved activity against gram-positive bacteria. *J. Biol. Chem. 276*, 24015–24022.
54. Carmieli, R., Papo, N., Zimmermann, H., Potapov, A., Shai, Y., and Goldfarb, D. (2006) Utilizing ESEEM spectroscopy to locate the position of specific regions of membrane-active peptides within model membranes. *Biophys. J. 90*, 492–505.
55. Zhu, W. L., Lan, H., Park, Y., Yang, S. T., Kim, J. I., Park, I. S., You, H. J., Lee, J. S., Park, Y. S., Kim, Y., Hahm, K. S., and Shin, S. Y. (2006) Effects of Pro → peptoid residue substitution on cell selectivity and mechanism of antibacterial action of tritrpticin-amide antimicrobial peptide. *Biochemistry 45*, 13007–13017.
56. Katsu, T., Ninomiya, C., Kuroko, M., Kobayashi, H., Hirota, T., and Fujita, Y. (1988) Action mechanism of amphipathic peptides gramicidin S and melittin on erythrocyte membrane. *Biochim. Biophys. Acta 939*, 57–63.
57. Matsuzaki, K., Murase, O., Fujii, N., and Miyajima, K. (1996) An antimicrobial peptide, magainin 2, induced rapid flip-flop of phospholipids coupled with pore formation and peptide translocation. *Biochemistry 35*, 11361–11368.
58. Brogden, K. A. (2005) Antimicrobial peptides: pore formers or metabolic inhibitors in bacteria? *Nat. Rev. Microbiol. 3*, 238–250.
59. Matsuzaki, K., Sugishita, K., Ishibe, N., Ueha, M., Nakata, S., Miyajima, K., and Epand, R. M. (1998) Relationship of membrane curvature to the formation of pores by magainin 2. *Biochemistry 37*, 11856–11863.
60. Matsuzaki, K., Sugishita, K., Harada, M., Fujii, N., and Miyajima, K. (1997) Interactions of an antimicrobial peptide, magainin 2, with outer and inner membranes of Gram-negative bacteria. *Biochim. Biophys. Acta 1327*, 119–130.
61. Yang, L., Harroun, T. A., Weiss, T. M., Ding, L., and Huang, H. W. (2001) Barrel-stave model or toroidal model? A case study on melittin pores. *Biophys. J. 81*, 1475–1485.
62. Tachi, T., Epand, R. F., Epand, R. M., and Matsuzaki, K. (2002) Position-dependent hydrophobicity of the antimicrobial magainin peptide affects the mode of peptide-lipid interactions and selective toxicity. *Biochemistry 41*, 10723–10731.
63. Shai, Y. (1999) Mechanism of the binding, insertion and destabilization of phospholipid bilayer membranes by alpha-helical antimicrobial and cell non-selective membrane-lytic peptides. *Biochim. Biophys. Acta 1462*, 55–70.
64. Lopes, J. L., Nobre, T. M., Siano, A., Humpola, V., Bossolan, N. R., Zaniquelli, M. E., Tonarelli, G., and Beltramini, L. M. (2009) Disruption of *Saccharomyces cerevisiae* by Plantaricin 149 and investigation of its mechanism of action with biomembrane model systems. *Biochim. Biophys. Acta 1788*, 2252–2258.
65. Galanth, C., Abbassi, F., Lequin, O., Ayala-Sanmartin, J., Ladram, A., Nicolas, P., and Amiche, M. (2009) Mechanism of antibacterial action of dermaseptin B2: interplay between helix-hinge-helix structure and membrane curvature strain. *Biochemistry 48*, 313–327.
66. Ambroggio, E. E., Separovic, F., Bowie, J. H., Fidelio, G. D., and Bagatolli, L. A. (2005) Direct visualization of membrane leakage induced by the antibiotic peptides: maculatin, citropin, and aurein. *Biophys. J. 89*, 1874–1881.